

Synchronization of Power Systems and Kuramoto Oscillators: A Regional Stability Framework

Lijun Zhu, and David J. Hill *Life Fellow, IEEE*

Abstract—The transient stability of power systems and synchronization of non-uniform Kuramoto oscillators are closely related problems. In this paper, we develop a novel regional stability analysis framework based on the proposed region-parametrized Lyapunov function to solve the problems. Also, a new synchronization definition is introduced and characterized by frequency boundedness and angle cohesiveness, the latter of which requires angles of any two connected nodes rather than any two arbitrary nodes to stay cohesive. It allows to take power fluctuations into explicit account as disturbances and can lead to less conservative stability condition. Applying the analysis framework, we derive two algebraic stability conditions for power systems that relate the underlying network topology and system parameters to the stability. Finally, to authors’ best knowledge, we first explicitly give the estimation of region of attraction for power systems. The analysis is verified via numerical simulation showing that two stability conditions can complement each other for predicting the stability.

I. INTRODUCTION

Power systems are a class of heterogeneous complex networks composed of load and generator buses connected via electric lines. The angle stability of power systems refers to the ability of bus angles to stay synchronism after severe faults or when the system experiences power fluctuations. It ensures stable and secure system operation to deliver electric power reliably from generators to loads. Small-disturbance and transient stability analysis are two classes of stability analysis. Small-disturbance stability concerns the stability issues of power systems under disturbances of small scale and usually uses the eigenvalue-based method following the model linearization. Transient stability considers the stability under rather large disturbances and the stability result is effective in a larger region of interest than the small-disturbance stability.

Transient stability assessment approaches are categorized into direct time-domain simulation and energy function methods. Time-domain simulation assesses the stability with respect to a given fault or disturbance by means of numerical simulation [18], [25]. On the contrary, the energy function method adopts Lyapunov stability theory and relies on a class of energy functions to determine the system stability. It identifies critical unstable equilibrium points (UEPs) [13] such as closest UEP or controlling UEP [7], [6] which are used to infer the stability. For instance, when the post-fault energy is less than the energy of closest UEP, the system

trajectory is guaranteed to converge towards the system equilibrium. Time-domain simulation is less intuitive and requires intensive computation especially for large-scale power systems but guarantees the accuracy if the precise modeling of the system is available [23], [24]. In comparison, energy function method provides more insights and is less computing intensive, although the estimated region of attraction is conservative.

The transient stability of power systems is also closely related to the synchronization of celebrated Kuramoto oscillators in terms of dynamic model and phase (angle) behavior. For conventional power systems, the dynamic model of synchronous generators under the over-damped assumption can be approximated by the modified Kuramoto model [11]. For microgrids, the droop-controlled frequency dynamics of the inverter-interfaced energy sources resemble Kuramoto model [1], [29], [30]. However, the network structures of Kuramoto oscillators and power networks sometimes are different. The complete graph structure is usually assumed for Kuramoto model and facilitates it to study necessary and sufficient synchronization conditions, while the network structure of power systems is usually irregular. In the early work, a network reduction method called Kron reduction ([20]) was introduced to simplify the network. For instance, reference [4], [22] considered loads were modeled as constant impedances and used Kron reduction to absorb loads into lines and reduce the original meshed power network into a network of generators. The Kron reduction simplifies the power network but has two drawbacks: the loss of the original topological information and inclusion of higher transfer conductances resulting from load absorption. The former makes it difficult to explore relation between stability and the original network topology, while the latter makes an unsolved problem to develop general Lyapunov functions. Later, Bergen and Hill [5] proposed the network-preserving model of conventional power systems with frequency-dependent loads for which Lyapunov functions in Lur’e-Postnikov form ([5], [15], [17]) were proposed. The network-preserving model allows for more precise dynamic modeling of loads, while the original network structure is retained.

The synchronization of Kuramoto oscillators refers to phase synchronization if natural frequencies of oscillators are identical or phase locking otherwise, i.e., phases of oscillators are distributed in a pattern. The phase locking coincides with transient stability definition of power systems. The research on Kuramoto oscillators mainly focus on finding necessary (see, e.g., [8], [31], [19]) and sufficient synchronization conditions (see, e.g., [8], [10], [14], [9]). The work [10], [11] first linked the stability of network-reduced power systems with syn-

This work was supported by The University of Hong Kong Research Committee Post-doctoral Fellow Scheme.

Lijun Zhu and David J. Hill are with Department of Electrical and Electronic Engineering, The University of Hong Kong, Hong Kong. (e-mail: ljzhu,dhill@eee.hku.hk).

chronization of Kuramoto oscillators, and adopted notations such as phase cohesiveness and frequency synchronization to characterize the stability for power systems. Motivated by [16], [11] also showed that the network topology has a crucial impact on the stability of power systems.

Over the last decade, the increasing integration of renewable energy into power grids has been motivated by environmental and economic benefits and continues as the enabling technology innovation progresses. Microgrid is one of promising technologies that can integrate large amount of renewable energy such as solar, wind power and geothermal systems, and fulfills the potential of distributed generation ([21], [26]) in a systematic way. In general, energy sources are fed via power-electronic converters, whose characteristics are determined by the internal control logic and are largely different from the conventional synchronous machine based power generators [29], [30], [27], [28]. The power generation of renewable energy is intermittent, stochastic and subjected to weather condition. On the other hand, the demand-side activities become complicated and less predictable. The generation of renewable energy and complicated load activities may cause fluctuations in power systems, which have not been accounted for in the existing stability analysis.

In this paper, we will show that the transient stability of power systems is related to the synchronization of non-uniform Kuramoto oscillators. The objective of this paper is to establish a general analysis framework based on energy (Lyapunov) functions to study the transient stability for power systems and the synchronization of non-uniform Kuramoto oscillators. The main contributions are summarized as follows. First, we introduce a new definition for the synchronization of power systems and Kuramoto oscillators characterized by angle differences across any physical lines being less than π , which complements the definition of phase cohesiveness in [11] that considers angle differences of any arbitrary two angles in the system. Second, with the recognition that renewable energy has stochastic and intermittent nature, we explicitly consider the energy fluctuations as disturbances to power systems and analyze their impact on stability. Third, we propose a general stability analysis method based on region-parametrized Lyapunov function whose bounds are parametrized by the size of region of interest. The stability analysis gives the existence condition of positively invariant sets in terms of the energy and boundedness in terms of the state which can be used to obtain the condition for angle cohesiveness and frequency boundedness. Fourth, applying the stability analysis framework, we derive two algebraic conditions for power systems in terms of the new definition and a definition similar to that in [11] that both relate the underlying network topology and system parameters to the stability. Finally, to authors' best knowledge, we first explicitly give the estimation of the region of attraction for power systems. This paper is a strengthened extension to our conference paper [33] in several aspects including the aforementioned third, fourth and last points. In addition, we will explain the motivation of the new synchronization definition using an example and show positively invariant set from bus angle perspective in addition to energy perspective in [33]. Also, we derive additional stability condition in Theorem

5.1.

The rest of the paper is structured as follows. Section II presents the structure-preserving model of power systems and introduces the first stability definition and describes the problem to be studied. In Section III, we introduce a new stability definition using a motivating example and present a coordinate transformation. In Section IV, we propose stability analysis framework based on region-parametrized Lyapunov functions and apply it to obtain two stability conditions for power systems in Section V. Section VI extends the stability analysis in Section V to non-disturbance scenario and explicitly gives the estimation of region of attraction for power systems. Section VII verifies theoretical results on the IEEE 9-bus test system using numerical simulation. The paper is concluded in Section VIII.

Notations. For a scalar $x \in \mathbb{R}$, $\text{sinc}(x) = \sin(x)/x$. For a vector $x = [x_1, \dots, x_n]^T \in \mathbb{R}^n$, $\|x\|$ and $\|x\|_\infty$ are the 2-norm and the ∞ -norm of vector x and $\sin(x) := [\sin(x_1), \dots, \sin(x_n)]^T$. The vector e_n is a column vector of dimension n with all elements being 1. The notations from algebraic graph theory is defined as follows. An undirected $\mathcal{G} = (\mathcal{V}, \mathcal{E})$ consists of a set of vertices $\mathcal{V} = \{1, \dots, n\}$ and a set of undirected edges $\mathcal{E} \subseteq \mathcal{V} \times \mathcal{V}$. An undirected edge of \mathcal{E} from node i to node j is denoted by (i, j) , meaning that nodes \mathcal{V}_i and \mathcal{V}_j are interconnected with each other. The edge weight is denoted by a_{ij} where $a_{ii} = 0$ and $a_{ij} = a_{ji} > 0$ for $(j, i) \in \mathcal{E}$. The Laplacian of the graph \mathcal{G} is denoted by $L = [l_{ij}] \in \mathbb{R}^{n \times n}$, where $l_{ii} = \sum_{j=1}^n a_{ij}$ and $l_{ij} = -a_{ij}$ if $i \neq j$. Denote by \mathcal{E}_k the k th edge of \mathcal{E} where $k \in \{1, \dots, |\mathcal{E}|\}$, $|\mathcal{E}|$ the number of edges, and $B \in \mathbb{R}^{n \times |\mathcal{E}|}$ the incidence matrix whose component is $B_{ik} = 1$ if node i is the sink node of edge \mathcal{E}_k , $B_{ik} = -1$ if it is the source node and $B_{ik} = 0$ otherwise. As a result, one can have $L = BA_v B^T$ where $A_v = \text{diag}(\{a_{ij}\}_{(i,j) \in \mathcal{E}})$ is the diagonal matrix with diagonal elements being edge weights. \mathcal{G}_c is called the complete graph induced by \mathcal{G} , if $\mathcal{G}_c = (\mathcal{V}, \mathcal{E}_c)$ is an undirected complete graph with the same set of nodes as \mathcal{G} , for which B_c is the incidence matrix.

II. SYSTEM MODEL AND PROBLEM FORMULATION

In this paper, we study the first-order dynamics

$$d_i \dot{\theta}_i = p_i(t) - \sum_{j=1}^n a_{ij} \sin(\theta_i - \theta_j), \quad i = 1, \dots, n. \quad (1)$$

The model (1) can represent Kuramoto oscillators, conventional power systems with over-damped synchronous generators [11], lossy [27] and lossless [1], [29] microgrids. For instance, the network-preserving model of lossless microgrids with inverter-based energy sources and loads can be described by (1) in which θ_i is the phase angle of the voltage V_i at bus i . The network parameter is $a_{ij} = |V_i| |V_j| |B_{ij}|$ where B_{ij} is the susceptance of the line connecting bus i and j , $|V_i|$ and $|V_j|$ are magnitudes of voltage V_i and V_j , respectively. Note that $a_{ij} > 0$ if two buses are connected, and $a_{ij} = 0$ otherwise. The net power injected from the network $p_{e,i} = -\sum_{j=1}^n a_{ij} \sin(\theta_i - \theta_j)$. Let $\mathcal{V} = \mathcal{V}_l \cup \mathcal{V}_s$ where $\mathcal{V}_l = 1, \dots, l$ and $\mathcal{V}_s = l + 1, \dots, n$ are index sets for the load

and energy source buses, respectively. For $i \in \mathcal{V}_l$, the equation (1) describes the power balance between power injection and power consumed by the load [1], for which we adopt the frequency-dependent load ([5]) where $p_i < 0$ is the nominal consumption and d_i is the frequency-dependent parameter. For $i \in \mathcal{V}_s$, energy sources are equipped with AC-AC or DC-AC inverter and their dynamics are determined by the internal control logic of the inverters which normally implement droop control [1] or maximum power point tracking (MPPT) [12]. For either control strategy, the equation (1) depicts the power balance between energy consumption by internal load, power supply by energy sources and power delivery to microgrids. For droop control, d_i and p_i are related to parameters and setpoints of the droop control (see [1]), while for MPPT control, p_i is the maximum power output and d_i is related to the internal frequency-dependent load. p_i can be simply regarded as the power supplied by i th energy source.

Remark 2.1: In contrast, the classic Kuramoto oscillators are

$$\dot{\theta}_i = p_i - \frac{K}{n} \sum_{j=1}^n \sin(\theta_i - \theta_j), \quad i = 1, \dots, n.$$

where p_i is the natural frequency of i th oscillator, K is the coupling strength and the network graph has all-to-all connections. The model (1) is also called non-uniform Kuramoto oscillators that was studied in [11]. Because the model (1) has non-complete interconnection and non-uniform coefficient d_i , it is more challenging to study the synchronization. ■

Remark 2.2: The model of lossy microgrids can also be written in the form of (1), with $p_i(t)$ replaced by $p'_i(t)$, as $d_i \dot{\theta}_i = p'_i(t) - \sum_{j=1}^n a_{ij} \sin(\theta_i - \theta_j)$, $i = 1, \dots, n$, where $p'_i(t) = p_i(t) - |V_i|^2 G_{ii} + \sum_{j=1}^n |V_i| |V_j| G_{ij} \cos(\theta_i - \theta_j)$. The second and last term in $p'_i(t)$ are the power transfer induced by non-zero conductances G_{ij} . This model can also represent the network-reduced model of conventional power systems with over-damped synchronous generators [11]. ■

The term p_i is normally assumed to be constant in the literature of power systems and Kuramoto oscillators, however it is worth mentioning that p_i in this paper might be time-varying due to load and renewable generation fluctuations. For instance, for MPPT control the maximum power outputs of the renewable energy such as PV and wind power normally vary with the weather condition.

The dynamical system (1) can be put in a vector form, with $\theta = [\theta_1, \dots, \theta_n]^T$, as follows

$$\dot{\theta} = -D^{-1} (BA_v \sin(B^T \theta) - p_f(t)) \quad (2)$$

where B is the incidence matrix of the power network \mathcal{G} , $D = \text{diag}(d_1, \dots, d_n)$ is the coefficient matrix, $p_f = [p_1, \dots, p_n]^T \in \mathbb{R}^n$ is called power profile vector. Define

$$\theta_c = B_c^T \theta, \quad (3)$$

where B_c is the incidence matrix of the induced complete graph \mathcal{G}_c . Hence, the elements in θ_c are $\theta_i - \theta_j$ for $i \neq j, \forall i, j \in \{1, \dots, n\}$. The stability in terms of synchronization for (2) with notations of phase cohesiveness and frequency

synchronization was introduced in [11], adapted in [32] and revised as follows. A few notations are adopted from [11] for the purpose of self-containedness. The torus is the set $\mathbb{T}^1 = [0, 2\pi]$ where 0 and 2π are associated with each other. An angle is a point $\theta \in \mathbb{T}^1$ and an arc is a connected subset of \mathbb{T}^1 . The n -torus is the Cartesian product $\mathbb{T}^n = \mathbb{T}^1 \times \dots \times \mathbb{T}^1$.

Definition 2.1: (Phase Cohesiveness and Frequency Boundedness). A solution $\theta(t) : \mathbb{R}^+ \rightarrow \mathbb{T}^n$ is then said to be phase cohesive if there exists a $\gamma \in [0, \pi)$ such that $\|\theta_c\|_\infty \leq \gamma$. A solution $\dot{\theta}(t) : \mathbb{R}^+ \rightarrow \mathbb{R}^n$ is then said to be frequency bounded if there exists a ϖ_o such that $\|\dot{\theta}(t)\|_\infty \leq \varpi_o$. ■

In [11], the transient stability of power systems and synchronization of non-uniform Kuramoto oscillators were studied in terms of phase cohesiveness and frequency synchronization, that is $\lim_{t \rightarrow \infty} \dot{\theta}(t) = ce_n$ for some constant $c \in \mathbb{R}$. Since p_i is time-varying in this paper, the system is not able to achieve the frequency synchronization but rather frequency boundedness in Definition 2.1. As shown in next section, the phase cohesiveness in Definition 2.1 may lead to some conservativeness and thus we will introduce a new phase cohesiveness definition later. The main *objective* of this paper is to investigate the synchronization of power systems and non-uniform Kuramoto oscillators (2) in the sense of Definition 2.1 and a new definition to be given in next section.

III. A NEW SYNCHRONIZATION DEFINITION AND EQUILIBRIUM SUBSPACE

A. A New Synchronization Definition

The notation of phase cohesiveness in the sense of Definition 2.1 was graphically explained in Example 2.2 of [10] for a two-bus system. The following example uses a three-bus system to complement the explanation in [10], explains the role of coupling forces between buses and more importantly motivates a new stability notation. A few more notations are helpful. For a set of angles $(\theta_1, \dots, \theta_n)$, define $\widehat{\theta_1 \dots \theta_n}$ the arc that starts at θ_1 , ends at θ_n and travels across angles in the order of $(\theta_1, \dots, \theta_n)$ and $\mathcal{A}(\widehat{\theta_1 \dots \theta_n})$ is its length.

Example 3.1: Consider the three-bus system (2) with zero power profile $p_i = 0$, $i = 1, \dots, 3$ and its network topology is illustrated in Fig. 1.b. The buses are labeled A, B, C and connected in an all-to-all fashion. As illustrated in Fig. 1.a, the bus angle in a torus is marked as a point in the circle. The desired synchronization behavior is that all three angles converge to a common value. Suppose, due to external disturbances, angle θ_C is disturbed to the position C_1 within arc \widehat{AB} . $\widehat{BAC_1}$ is the shortest arc containing all $(\theta_A, \theta_B, \theta_C)$ in its interior and $\mathcal{A}(\widehat{BAC_1}) < \pi$. In this case, the coupling forces among them play an active role of holding bus angles together. No matter angle θ_C leads ahead/lags behind angle θ_A , it will result in negative/positive coupling force $-a_{CA} \sin(\theta_C - \theta_A)$ at bus C , decelerating/accelerating the angle θ_C to force these two angles together. This argument also applies to angle pairs (A, B) and (B, C) . As a result, the length of the arc stays $\mathcal{A}(\widehat{BAC_1}) < \pi$, and then angles are cohesive in the sense of Definition 2.1. This mechanism

is effective if $\mathcal{A}(\widehat{BAC_1}) < \pi$ which coincides with the cohesiveness condition $\max_{i,j \in \{A,B,C\}} |\theta_i - \theta_j| \leq \gamma < \pi$. However, if θ_c is disturbed farther away beyond the position B' to the position C_2 in Fig. 1.a, say within $\widehat{B'A'}$. By definition, the phase cohesiveness in Definition 2.1 does not cover this case, since the shortest arc containing all $(\theta_A, \theta_B, \theta_C)$ and with length less than π does not exist. Let us explain it in terms of coupling forces. When the angle of bus C is at C_2 , the coupling forces that applies from B (simply illustrated by f_{BC} in Fig. 1.a) and that applies from A (illustrated by f_{AC}) counteract with each other. Hence, whether three angles converge to a common value becomes indeterminate.

Then, consider buses A, B, C are connected in a way illustrated in Fig. 1.c. As known, the coupling forces only exist between bus A and bus B and between bus A and bus C . Suppose C is at position C_2 for which phase cohesiveness in Definition 2.1 fails to infer the stability. However, it is observed that the coupling forces between A and B and between A and C , tends to attract B and C towards A , making the region $\widehat{BAC_2}$ contract and showing it is potentially stable.

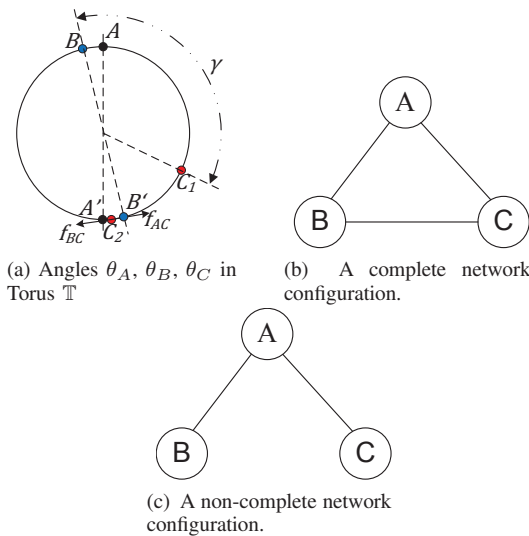


Fig. 1. Illustration of phase cohesiveness for the power system in different network configurations.

The observation in Example 3.1 motivates us to propose a different definition of phase cohesiveness that is concerned with angle differences across lines. Define

$$\theta_l = B^T \theta, \quad (4)$$

where B is the incidence matrices of the graph \mathcal{G} . Each element in θ_l is angle difference across the corresponding physical line.

Definition 3.1: (Phase Cohesiveness and Frequency Boundedness). A solution $\theta(t) : \mathbb{R}^+ \rightarrow \mathbb{T}^n$ is then said to be phase cohesive if there exists a $\gamma \in [0, \pi)$ such that $\|\theta_l\|_\infty \leq \gamma$. A solution $\dot{\theta}(t) : \mathbb{R}^+ \rightarrow \mathbb{R}^n$ is then said to be frequency bounded if there exists a ϖ_o such that $\|\dot{\theta}(t)\|_\infty \leq \varpi_o$.

As a result, the second case in Example 3.1 could be phase cohesive in the sense of Definition 3.1. When \mathcal{G} is a

complete graph, $\max_{i,j \in \{1, \dots, n\}} |\theta_i - \theta_j| \leq \gamma$ is equivalent to $\max_{(i,j) \in \mathcal{V}} |\theta_i - \theta_j| \leq \gamma$ and therefore Definition 3.1 coincides with Definition 2.1. It is worth noting that considering the system behavior of θ in Euclidean Space \mathbb{R}^n and in Torus \mathbb{T}^n is equivalent as far as the initial condition $\theta(t_o) \in \mathbb{R}^n$ at $t = t_o$ satisfies $\max_{(i,j) \in \mathcal{E}} |\theta_i(t_o) - \theta_j(t_o)| \leq \gamma$ or $\max_{(i,j) \in \{1, \dots, n\}} |\theta_i(t_o) - \theta_j(t_o)| \leq \gamma$.

B. Coordinate Transformation and Equilibrium Subspace

For the operation of classic power systems and microgrids, the load demand and the generation of non-dispatchable energy sources are predicted. They are fed into the optimal power flow algorithm to calculate the power required to be generated at dispatchable energy sources in order to meet economic goals and system operation requirements. The scheduled power generation matches the predicted demand and their relation is described by the power flow equation

$$BA_v \sin(B^T \theta_e) = p_o, \quad (5)$$

with

$$\theta_e := \theta_o + ce_n \quad (6)$$

where p_o is a vector consisting of predicted load demand and scheduled power generation satisfying $e_n^T p_o = 0$. $\theta_o = \text{col}(\theta_1^o, \dots, \theta_n^o) \in \mathbb{R}^n$ is a constant vector that characterizes the relative angle differences among buses and $c \in \mathbb{R}$ is an arbitrary constant capturing the uniform angle offset on every bus. Since the uniqueness of equilibria is fully described by θ_o , in what follows, we call θ_o equilibrium point for simplicity.

In fact, the real-time power profile p_f might not align with the scheduled p_o , due to the load and renewable generation fluctuations caused by complicated load activity and the variation of the weather condition. Let $p(t) = p_f(t) - p_o$ be the power deviation from the dispatched power profile and regarded as the disturbance to power systems when the system is scheduled to operate around the equilibrium point θ_o . Let

$$\delta_i = \theta_i - \theta_i^o \quad (7)$$

be the angle deviation from the equilibrium point. The dynamical system (2) can be rewritten in the new coordinate as follows

$$\begin{aligned} \dot{\delta} &= -D^{-1} (BA_v (\sin(B^T(\delta + \theta_o)) \\ &\quad - \sin(B^T \theta_o)) - p(t)) \end{aligned} \quad (8)$$

where $\delta = [\delta_1, \dots, \delta_n]^T \in \mathbb{R}^n$. The equilibrium subspace for the system (8) is

$$\mathbb{E} := \{\delta \in \mathbb{R}^n \mid \delta = ce_n, \forall c \in \mathbb{R}\} \quad (9)$$

on which angle deviations are synchronized, i.e., $\delta_i - \delta_j = 0$, $\forall i, j = \{1, \dots, n\}$. As a result, the stability with respect to an equilibrium point θ_o is converted into the stability with respect to this equilibrium subspace \mathbb{E} .

Denote $\delta_c = B_c^T \delta$ and

$$\bar{\delta}_c = \max_{i,j=1, \dots, n} \{|\theta_i^o - \theta_j^o|\}, \quad (10)$$

With the coordinate transformation (7), we present weakened versions of Definition 2.1 and 3.1, respectively.

Definition 3.2: (Synchronization I) A solution $\delta(t) : \mathbb{R}^+ \rightarrow \mathbb{R}^n$ is then said to be phase cohesive if there exists a $\gamma \in [0, \pi - \bar{\delta}_c)$ such that $\|\delta_c(t)\|_\infty \leq \gamma$. A solution $\dot{\delta}(t) : \mathbb{R}^+ \rightarrow \mathbb{R}^n$ is then said to be frequency bounded if there exists a ϖ_o such that $\|\dot{\delta}(t)\|_\infty < \varpi_o$. ■

Similarly, denote $\delta_l = B^T \delta$ and

$$\bar{\delta}_l = \max_{(i,j) \in \mathcal{E}} \{|\theta_i^o - \theta_j^o|\}. \quad (11)$$

The phase cohesiveness and frequency boundedness in Definition 3.1 can be given in terms of δ_l .

Definition 3.3: (Synchronization II) A solution $\delta(t) : \mathbb{R}^+ \rightarrow \mathbb{R}^n$ is then said to be phase cohesive if there exists a $\gamma \in [0, \pi - \bar{\delta}_l)$ such that $\|\delta_l(t)\|_\infty \leq \gamma$. A solution $\dot{\delta}(t) : \mathbb{R}^+ \rightarrow \mathbb{R}^q$ is then said to be frequency bounded if there exists a ϖ_o such that $\|\dot{\delta}(t)\|_\infty < \varpi_o$. ■

Since $|\theta_i^o - \theta_j^o| \leq c_1$ and $|\delta_i - \delta_j| \leq c_2$ imply $|\theta_i - \theta_j| \leq c_1 + c_2$ for $c_1 + c_2 \leq \pi$, the phase cohesiveness and frequency boundedness in Definition 3.2 and Definition 3.3 implies that in Definition 2.1 and 3.1, respectively. Therefore, they are weakened versions of Definition 2.1 and 3.1. In fact, taking $(\theta_o, p_o) = (0, 0)$ in (5) results in $\delta = \theta$, $p = p_f$ and $\bar{\delta}_l = \bar{\delta}_c = 0$ which in turn recovers θ -dynamics (2) from δ -dynamics (8). In the sequel, we will mainly focus on the stability analysis in the sense of Definition 3.2 and 3.3 and the analysis can be easily extended to Definition 2.1 and 3.1 by taking $(\theta_o, p_o) = (0, 0)$. In this paper, we have the following assumption.

Assumption 3.1: $\bar{\delta}_l < \pi/2$. ■

Note that this is a reasonable assumption for power systems, since the secure operation is assured when the angle difference across any physical line is less than $\pi/2$.

IV. REGIONAL STABILITY ANALYSIS FRAMEWORK

In this section, we will present a novel regional stability analysis framework that will be applied to explore the stability of power systems in the sense of Definition 3.2 and 3.3. Consider a nonlinear system

$$\dot{x} = f(t, x) \quad (12)$$

where $x \in \mathbb{R}^n$ is the state and the origin is the equilibrium point of the system (12), i.e., $f(t, 0) = 0$. Define the compact set $B(r) := \{x \in \mathbb{R}^n \mid \|x\| \leq r\}$. The analysis is based on the region-parametrized Lyapunov function defined as follows.

Definition 4.1: A continuously differentiable function $V(x) : B(r_m) \rightarrow \mathbb{R}^+$ is called a region-parametrized Lyapunov function (RPLF) if for any given region $\gamma \in [0, \gamma_m]$, there exist non-negative functions $\underline{\alpha}$, $\bar{\alpha}$ and μ such that for $\|x\| \leq \gamma$ it holds that

$$\underline{\alpha}(\gamma)\|x\|^2 \leq V(x) \leq \bar{\alpha}(\gamma)\|x\|^2, \quad (13)$$

$$\frac{\partial V}{\partial x} f(t, x) < 0, \quad \forall \|x\| \geq \mu(\gamma). \quad (14)$$

Remark 4.1: Note that bounds of the RPLF and the condition for its time derivative to be negative are parametrized by the size γ of the region to be considered. When the system admits a Lyapunov function $\tilde{V}(x) : D \rightarrow \mathbb{R}^+$ where $D \in B(r_m) \in \mathbb{R}^n$ satisfying $\underline{\phi}(\|x\|) \leq \tilde{V}(x) \leq \bar{\phi}(\|x\|)$ with class \mathcal{K} functions $\underline{\phi}$ and $\bar{\phi}$, we can use \tilde{V} as the RPLF candidate and explicitly calculate the bounds in (13). If $\lim_{s \rightarrow 0} s^2/\underline{\phi}(s) < \infty$ and $\lim_{s \rightarrow 0} \bar{\phi}(s)/s^2 < \infty$, one can choose $\bar{\alpha}(\gamma) = \sup_{\|x\| \leq \gamma} \{\bar{\phi}(\|x\|)/\|x\|^2\}$, $\underline{\alpha}(\gamma) = \inf_{\|x\| \leq \gamma} \{\underline{\phi}(\|x\|)/\|x\|^2\}$. ■

The next lemma establishes the condition on which we can find a positively invariant set within the region $\|x(t)\| \leq \gamma_m$ when there exists a RPLF. It can be used to investigate the condition for the phase cohesiveness in Definition 3.2 and 3.3. Before proceeding, let us define the compact set $W(r) := \{x \in \mathbb{R}^n \mid V(x) \leq r\}$ with V as a RPLF.

Lemma 4.1: Consider nonlinear system (12). Suppose there exists a RPLF $V(x)$ defined for $\|x\| \leq \gamma_m$. For a given $\gamma \in [0, \gamma_m]$, if it holds that

$$g(\gamma) := \frac{\gamma}{\mu(\gamma)} \sqrt{\frac{\bar{\alpha}(\gamma)}{\underline{\alpha}(\gamma)}} \geq 1, \quad (15)$$

then there exists a $\chi \in \mathbb{R}$ satisfying $f_l(\gamma) \leq \chi \leq f_r(\gamma)$ with

$$f_l(\gamma) := \bar{\alpha}(\gamma)\mu^2(\gamma), \quad f_r(\gamma) := \gamma^2\underline{\alpha}(\gamma) \quad (16)$$

such that $W(\chi)$ is a positively invariant set, i.e., any trajectories starting with $x(t_o) \in W(\chi)$ is ultimately contained in $W(f_l(\gamma))$ and along the trajectory $\|x\| \leq \gamma$ holds. ■

Proof: See Appendix. ■

Definition 4.2: A positive continuous function $g(\gamma) : D = \{\gamma \mid 0 \leq \gamma \leq \gamma_m\} \rightarrow \mathbb{R}^+$ is called a quasi-sinusoidal function if $g(0) = 0$, $g(\gamma_m) = 0$ and $g(\gamma)$ monotonically increases with x for $0 \leq \gamma \leq \gamma^*$ and monotonically decreases with γ for $\gamma^* < \gamma \leq \gamma_m$ where $r^* = \arg \max_{\gamma \in D} \{g(\gamma)\}$. ■

The next lemma gives the sufficient condition under which the solution to the inequality (15) exists and further elaborates the result in Lemma 4.1 provided that $g(\gamma)$ in (15) is a quasi-sinusoidal function.

Lemma 4.2: Consider nonlinear system (12) and there exists a RPLF $V(x)$ defined for $\|x\| \leq \gamma_m$. Suppose $g(\gamma)$ in (15) is a quasi-sinusoidal function of $\gamma \in [0, \gamma_m]$ and maximized at $\gamma = \gamma^*$. If $g(\gamma^*) > 1$, then

- there exists $0 < \gamma_{\min} < \gamma^*$ and $\gamma^* < \gamma_{\max} < \gamma_m$ such that $g(\gamma_{\min}) = 1$, $g(\gamma_{\max}) = 1$ and $g(\gamma) > 1$ for $\gamma \in (\gamma_{\min}, \gamma_{\max})$;
- (Energy Perspective) if $f_l(\gamma)$ is a monotonically increasing function of γ , $W(\chi)$ is a positively invariant set for every $\chi \in [f_{l,\min}, f_{r,\max}]$ where $f_{l,\min} = f_l(\gamma_{\min})$ and $f_{r,\max} = \max_{\gamma \in [\gamma_{\min}, \gamma_{\max}]} \{f_r(\gamma)\}$. Moreover, any trajectories starting within $x(t_o) \in W(\chi)$ is ultimately contained in $W(f_{l,\min})$;

C. (State Perspective) let

$$\begin{aligned}\gamma_l &= \min_{\gamma \in [\gamma_{\min}, \gamma_{\max}]} \left\{ \sqrt{\frac{f_{l,\min}}{\underline{\alpha}(\gamma)}} \left| \frac{f_{l,\min}}{\underline{\alpha}(\gamma)} \leq \gamma^2 \right. \right\}, \\ \gamma_r &= \max_{\gamma \in [\gamma_{\min}, \gamma_{\max}]} \left\{ \sqrt{\frac{f_{r,\max}}{\bar{\alpha}(\gamma)}} \left| \frac{f_{r,\max}}{\bar{\alpha}(\gamma)} \leq \gamma^2 \right. \right\}.\end{aligned}\quad (17)$$

Then, any trajectory starting within $B(\gamma)$ for $\gamma \in [\gamma_l, \gamma_r]$ is ultimately contained in $B(\gamma_l)$.

Proof: See Appendix. ■

V. SYNCHRONIZATION AND TRANSIENT STABILITY ANALYSIS

In this section, we will explore the synchronization of power systems (8) by proposing a class of parameterized energy functions as the RPLFs.

A. Energy Functions

The model of microgrids can be rewritten as

$$\dot{\delta} = F\delta - G\psi(H^T\delta) + Gp \quad (18)$$

where

$$\psi(H^T x) = BA_v (\sin(B^T(\delta + \theta_o)) - \sin(B^T\theta_o)) \quad (19)$$

and

$$F = 0, \quad G = D^{-1}, \quad H = I. \quad (20)$$

The equation (18) with $p = 0$ is similar to Lur'e form except that it is not a minimal realization and under-actuated, due to $e_n^T \psi(H^T x) = 0$. Let us propose a general class of energy function

$$V(\delta) = V_1(\delta) + V_2(\delta) \quad (21)$$

where

$$V_1(\delta) = \frac{1}{2} \alpha \delta^T P \delta \quad (22)$$

$$\begin{aligned}V_2(\delta) &= \frac{1}{2} \beta \sum_{i=1}^n \sum_{j=1}^n a_{ij} \int_0^{\delta_i - \delta_j} [\sin(u + \theta_i^o - \theta_j^o) \\ &\quad - \sin(\theta_i^o - \theta_j^o)] du.\end{aligned}\quad (23)$$

with $P \in \mathbb{R}^{n \times n}$ and $\alpha, \beta \in \mathbb{R}$ to be determined.

The following proposition is inspired by the work [3], [15] and cited from [32], which is used to choose P , α and β .

Proposition 5.1: ([32]) Consider the dynamic system (18) or equivalently the microgrids (8) with $p = 0$. If there exist a symmetric matrix P and matrices L , W , and X of proper dimensions such that the following equalities are satisfied

$$\begin{aligned}PF + F^T P &= -LL^T \\ PG &= \alpha H + \beta F^T H - LW + X e_n^T \\ W^T W &= \beta(H^T G + G^T H),\end{aligned}\quad (24)$$

then the energy function V in (21) satisfies $\dot{V} \leq 0$ for $|\delta_i - \delta_j| < \pi - 2\bar{\delta}_l, \forall (i, j) \in \mathcal{E}$ where $\bar{\delta}_l$ is defined in (11). ■

Proof: The proof is similar to that in [3], [15], [32] and hence is omitted here. ■

According to (24) and entities in (20), we follow the procedure presented in [15] and find that $\alpha > 0$, $\beta > 0$ can be selected arbitrarily and

$$P = (D - De_n e_n^T D/d) \quad (25)$$

where $d = e_n^T D e_n$ such that (24) is satisfied and the energy function (21) obtains $V = 0$ at equilibrium subspace \mathbb{E} defined in (9). It will be shown that the energy function (21) is a RPLF for power systems (8) in the sense of Definition 4.1. Let us define functions

$$\kappa(\gamma) := \text{sinc}(\gamma/2) \cos(\gamma/2 + \bar{\delta}_l). \quad (26)$$

where $\bar{\delta}_l$ is given in (11) and

$$f(\gamma) = \gamma^q \kappa^p(\gamma) \quad (27)$$

Two more lemmas are needed before we proceed to explore the synchronization and transient stability of power systems.

Lemma 5.1: ([32]) $\kappa(\gamma)$ is a monotonically decreasing function and $f(\gamma)$ is a quasi-sinusoidal function in the sense of Definition 4.2, obtains zeros at $\gamma = 0, \pi - 2\bar{\delta}_l$ and reaches its maximum at $\gamma = \gamma^*$ satisfying

$$p \cos(\gamma^* + \bar{\delta}_l) = (p - q) \kappa(\gamma^*). \quad (28)$$

where $\gamma^* < \pi/2 - \bar{\delta}_l$ if $p > q$. ■

Lemma 5.2: ([2]) For Hermitian nonnegative definite matrices X and Y with ordered eigenvalues, i.e., $\lambda_1(X) \geq \dots \geq \lambda_n(X)$ and $\lambda_1(Y) \geq \dots \geq \lambda_n(Y)$, it holds that

$$\lambda_{i+j-1}(XY) \leq \lambda_j(X) \lambda_i(Y), \quad i + j \leq n + 1, \quad (29)$$

$$\lambda_{i+j-n}(XY) \geq \lambda_j(X) \lambda_i(Y), \quad i + j \geq n + 1. \quad (30)$$

where $1 \leq i, j \leq n$. ■

B. Synchronization Criterion I

In this subsection, we use the energy function (21) with $\alpha = 1$, $\beta = 0$ and P specified in (25). The energy function is repeated as follows

$$V = \frac{1}{2} \delta^T (D - De_n e_n^T D/d) \delta. \quad (31)$$

Due to $2(D - De_n e_n^T D/d) = \sum_{i=1}^n \sum_{j=1}^n d_i d_j (\delta_i - \delta_j)^2$, the energy function is similar to the one used in [11] where the energy function is however defined in the original θ -coordinate. The difference is due to that the synchronization condition to be derived for power systems (8) is given in the angle-deviation δ -coordinate instead of the original system (2). We will adopt the regional stability analysis method presented in Section IV. Then, the synchronization condition in the sense of Definition 3.2 is presented by the following theorem with the notation $B_c(\gamma) := \{\delta_c \in \mathbb{R}^{(n-1)n/2} \mid \|\delta_c\| \leq \gamma\}$.

Theorem 5.1: Consider power systems (8) with energy function (31) under Assumption 3.1. Assume $\bar{\delta}_c - \bar{\delta}_l < \pi/2$.

Let $\gamma \in [0, \pi - \bar{\delta}_m)$ where $\bar{\delta}_m = \max\{2\bar{\delta}_l, \bar{\delta}_c\}$ and $\kappa(\gamma)$ be defined in (26). Let function $\sigma(\gamma)^1$ be

$$\sigma(\gamma) = \sqrt{\frac{\max_{i \neq j}\{d_i d_j\}}{\min_{i \neq j}\{d_i d_j\}}} \times \frac{n \|\text{diag}\{d_i d_j\} B_c^T D^{-1} p(t)\|_{[t_0, \infty]}}{\gamma \kappa(\gamma) d}. \quad (32)$$

If it holds that

$$\lambda_2 > \lambda_{cr} := \sigma(\gamma^*), \quad (33)$$

where λ_2 is the algebraic connectivity of the underlying Laplacian L of power network and $\gamma^* = \pi/2 - \bar{\delta}_l$, the synchronization in the sense of Definition 3.2 is achieved. In particular,

- A. there exists $0 < \gamma_{\min} < \pi/2 - \bar{\delta}_l$ and $\pi/2 - \bar{\delta}_l < \gamma_{\max} < \pi - \bar{\delta}_m$ such that $\lambda_2 = \sigma(\gamma_{\min})$, $\lambda_2 = \sigma(\gamma_{\max})$ and $\lambda_2 > \sigma(\gamma)$ for $\gamma \in (\gamma_{\min}, \gamma_{\max})$;
- B. (Energy Perspective) $W(\chi)$ is a positively invariant set for any $\chi \in [f_{l, \min}, f_{r, \max}]$ where

$$f_{l, \min} = \gamma_{\min}^2 \min_{i \neq j}\{d_i d_j\} / (2d), \quad (34)$$

$$f_{r, \max} = \gamma_{\max}^2 \min_{i \neq j}\{d_i d_j\} / (2d), \quad (35)$$

i.e., any trajectories δ starting within $x(t_0) \in W(\chi)$ is ultimately contained in $W(f_{l, \min})$;

- C. (Angle Perspective: phase cohesiveness) let

$$\gamma_l = \gamma_{\min}, \gamma_r = \gamma_{\max} \sqrt{\frac{\min_{i \neq j}\{d_i d_j\}}{\max_{i \neq j}\{d_i d_j\}}}. \quad (36)$$

Then, any trajectories $\delta(t)$ starting within $B_c(\gamma)$ for $\gamma \in [\gamma_l, \gamma_r]$ is ultimately contained in $B_c(\gamma_l)$.

- D. (Frequency Boundedness) if p is bounded, there exists a T such that $\|\dot{\delta}\|_{\infty} \leq \varpi_o$ for some ϖ_o and $t > T$.

■

Proof: First, we will verify the energy function $V(\delta)$ in (31) is a RPLF. Note that

$$(D - De_n e_n^T / d) = B_c \text{diag}\{d_i d_j\} B_c^T / d \quad (37)$$

where B_c is the incidence matrix of the induced complete graph. It leads to

$$\underline{\alpha} \|\delta_c\| \leq V \leq \bar{\alpha} \|\delta_c\| \quad (38)$$

where $\delta_c = B_c \delta$ and

$$\underline{\alpha} = \min_{i \neq j}\{d_i d_j\} / (2d), \quad \bar{\alpha} = \max_{i \neq j}\{d_i d_j\} / (2d). \quad (39)$$

For the rest of the proof, we consider Lyapunov function V within $\|\delta_c\| \leq \gamma$ for $\gamma \in [0, \pi - 2\bar{\delta}_l)$. Note that $\|\delta_l\|_{\infty} \leq \|\delta_c\|_{\infty} \leq \|\delta_c\| \leq \gamma$ implies that $|\delta_i - \delta_j| \leq \gamma$, $\forall (i, j) \in \mathcal{E}$. The derivative of $V(\delta)$, along the trajectory of (8), is

$$\begin{aligned} \dot{V} &= \delta^T (I - De_n e_n^T / d) p \\ &\quad - BA_v (\sin(B^T(\delta + \theta_o)) - \sin(B^T \theta_o)) \\ &= -\delta^T BA_v (\sin(B^T(\delta + \theta_o)) - \sin(B^T \theta_o)) \\ &\quad + \delta^T (I - De_n e_n^T / d) p. \end{aligned} \quad (40)$$

¹For convenience, we denote $\|s(t)\|_{[t_1, t_2]} = \sup_{t_1 \leq t \leq t_2} \|s(t)\|$ for a bounded vector singular $s(t)$.

Since $|\delta_i - \delta_j| \leq \gamma$ and $\|\theta_i^o - \theta_j^o\| \leq \bar{\delta}_l$ for any bus j that is connected with bus i , one has

$$\begin{aligned} &\frac{\sin(\delta_i - \delta_j + \theta_i^o - \theta_j^o) - \sin(\theta_i^o - \theta_j^o)}{\delta_i - \delta_j} \\ &= \frac{\cos((\delta_i - \delta_j)/2 + \theta_i^o - \theta_j^o) \sin((\delta_i - \delta_j)/2)}{(\delta_i - \delta_j)/2} \geq \kappa(\gamma) \end{aligned}$$

where $\kappa(\gamma)$ is defined in (26). As a result,

$$\begin{aligned} \delta^T BA_v (\sin(B^T(\delta + \theta_o)) - \sin(B^T \theta_o)) &= \frac{1}{2} \sum_{i=1}^n \sum_{j=1}^n [a_{ij} (\delta_i - \delta_j)^2 \\ &\quad \frac{\sin(\delta_i - \delta_j + \theta_i^o - \theta_j^o) - \sin(\theta_i^o - \theta_j^o)}{\delta_i - \delta_j}] \\ &\geq \kappa(\gamma) \delta^T \mathcal{L} \delta \geq \frac{\lambda_2}{n} \kappa(\gamma) \|\delta_c\|^2, \end{aligned}$$

where the last inequality is due to Lemma 4.7 in [11] and

$$\delta^T (I - De_n e_n^T / d) p = \delta_c \text{diag}\{d_i d_j\} B_c^T D^{-1} p / d.$$

where we used (37). Equation (40) leads to

$$\begin{aligned} \dot{V} &\leq -\frac{\lambda_2}{n} \kappa(\gamma) \|\delta_c\|^2 + \delta_c \text{diag}\{d_i d_j\} B_c^T D^{-1} p / d \\ &\leq 0, \text{ if } \|\delta_c\| \geq \frac{n \|\text{diag}\{d_i d_j\} B_c^T D^{-1} p(t)\|_{[t_0, \infty]}}{\kappa(\gamma) \lambda_2 d}. \end{aligned}$$

So far, we concluded that V is a RPLF. Then, if

$$g(\gamma) := \gamma \kappa(\gamma) / R_s \geq 1, \quad (41)$$

where

$$\begin{aligned} R_s &:= \sqrt{\frac{\max_{i \neq j}\{d_i d_j\}}{\min_{i \neq j}\{d_i d_j\}}} \\ &\quad \times \frac{n \|\text{diag}\{d_i d_j\} B_c^T D^{-1} p(t)\|_{[t_0, \infty]}}{\lambda_2 d}, \end{aligned} \quad (42)$$

the condition of Lemma 4.1 is satisfied. We further analyze the inequality (41) using Lemma 4.2. Note that $g(\gamma)$ in (41) is a quasi-sinusoidal function and maximizes at $\gamma^* = \pi/2 - \bar{\delta}_l$ by Lemma 5.1. If $g(\gamma^*) > 1$ which is equivalent to (33), it follows from Statement A of Lemma 4.2 that Statement A is satisfied. We can calculate $f_{l, \min}$ in Lemma 4.2 as

$$f_{l, \min} = \frac{n^2 \|\text{diag}\{d_i d_j\} B_c^T D^{-1} p(t)\|_{[t_0, \infty]}^2 \max_{i \neq j}\{d_i d_j\}}{2 \kappa^2(\gamma_{\min}) \lambda_2^2 d^3} \quad (43)$$

and $f_{r, \max} = \underline{\alpha} \gamma_{\max}^2$. Noting $\lambda_2 = \sigma(\gamma_{\min})$ and $\underline{\alpha}$ in (39), we can obtain the neat expression of $f_{l, \min}$ in (34) and $f_{r, \max}$ in (35). As a result, Statement B follows that of Lemma 4.2. Statement C follows from that of Lemma 4.2 by noting functions $\underline{\alpha}(\gamma)$ and $\bar{\alpha}(\gamma)$ do not depend on γ .

What remains is to prove frequency boundedness. Statement C implies that there exists a T such that the system trajectory $\delta_c(t)$ enters and stay in the ball $B(\gamma_l)$ for $t > T$ where $\gamma_l = \gamma_{\min} < \gamma^* = \pi/2 - \bar{\delta}_l$. We also note $\|\delta_c\| \leq \gamma_l = \gamma_{\min} < \pi/2 - \bar{\delta}_l$ implies that $|\delta_i - \delta_j + \theta_i^o - \theta_j^o| < \frac{1}{2}\pi$. As a result, RHS of (8) is bounded, which shows that $\|\dot{\delta}\|$ is bounded. So, the frequency $\dot{\delta}$ will be ultimately bounded, i.e., $\|\dot{\delta}(t)\| \leq \varpi_o$ for $t > T$ with some ϖ_o and T . The frequency boundedness is proved. ■

Taking $(\theta_o, p_o) = (0, 0)$ in (5) recovers θ -dynamics (2) from δ -dynamics (8) and makes $\kappa(\gamma) = \sin(\gamma)/\gamma$. As a result, the energy function becomes $V = \theta^T(D - De_n e_n^T D/d)\theta$ which coincides with the one used in [11]. Then, we arrive at the following corollary with this energy function.

Corollary 5.1: Consider microgrid (2) with energy function $V = \theta^T(D - De_n e_n^T D/d)\theta$. Let $\gamma \in [0, \pi)$ and function $\bar{\sigma}(\gamma)$ be

$$\bar{\sigma}(\gamma) = \sqrt{\frac{\max_{i \neq j} \{d_i d_j\} / \min_{i \neq j} \{d_i d_j\}}{n \|\text{diag}\{d_i d_j\} B_c^T D^{-1} p(t)\|_{[t_0, \infty]}}} \times \frac{1}{\sin(\gamma) d}$$

If $\lambda_2 > \lambda_{cr} := \bar{\sigma}(\gamma^*)$ holds where $\gamma^* = \pi/2$, the synchronization in the sense of Definition 2.1 is achieved. In particular,

- there exists $0 < \gamma_{\min} \leq \pi/2$ and $\pi/2 < \gamma_{\max} < \gamma_{\max}$ such that $\lambda_2 = \bar{\sigma}(\gamma_{\min})$, $\lambda_2 = \bar{\sigma}(\gamma_{\max})$ and $\lambda_2 > \lambda_{cr}$ for $\gamma \in (\gamma_{\min}, \gamma_{\max})$;
- (Energy Perspective) $W(\chi)$ is a positively invariant set for any $\chi \in [f_{l, \min}, f_{r, \max}]$ where

$$f_{l, \min} = \gamma_{\min}^2 \min_{i \neq j} \{d_i d_j\} / (2d), \quad (44)$$

$$f_{r, \max} = \gamma_{\max}^2 \min_{i \neq j} \{d_i d_j\} / (2d), \quad (45)$$

i.e., any trajectories θ starting within $x(t_o) \in W(\chi)$ is ultimately contained in $W(f_{l, \min})$;

- (Angle Perspective: phase cohesiveness) let

$$\gamma_l = \gamma_{\min}, \gamma_r = \gamma_{\max} \sqrt{\frac{\min_{i \neq j} \{d_i d_j\}}{\max_{i \neq j} \{d_i d_j\}}}. \quad (46)$$

Any trajectories θ starting within $B_c(\gamma)$ for $\gamma \in [\gamma_l, \gamma_r]$ is ultimately contained in $B_c(\gamma_l)$.

- if p is bounded, there exists a T such that $\|\dot{\theta}\|_\infty \leq \varpi_o$ for some ϖ_o and $t > T$.

Remark 5.1: Statement A and C in Corollary 5.1 coincide with Theorem 4.4 in [11] where constant power profile p_f is considered and frequency synchronization can be achieved. As we consider some entries in power profile are time-varying, Corollary 5.1 extends the result in [11] to frequency boundedness in Statement D and in addition provide the existence of the invariant set from energy perspective in Statement B. Also, the condition is derived using the regional stability analysis method proposed in Section IV. ■

C. Synchronization Criterion II

In this subsection, we use the energy function (21) with $\alpha = 0$ and $\beta = 1$ which is repeated as follows

$$V(\delta) = \frac{1}{2} \sum_{i=1}^n \sum_{j=1}^n a_{ij} \int_0^{\delta_i - \delta_j} (\sin(u + \theta_{ij}^o) - \sin \theta_{ij}^o) du. \quad (47)$$

where $\theta_{ij}^o = \theta_i^o - \theta_j^o$. In fact, $V(\delta)$ is the sum of the potential energy induced by the coupling force between i th bus and j th bus when angles move away from the equilibrium θ_o . Since

$a_{ij} \neq 0$ if and only if $(i, j) \in \mathcal{E}$, $V(\delta)$ sums up the potential energy only induced across transmission lines.

Lemma 5.3: For a given $\gamma \in [0, \pi - 2\bar{\delta}_l)$, if $\max_{(i,j) \in \mathcal{E}} |\delta_i - \delta_j| \leq \gamma$, then

$$\underline{\alpha}(\gamma) \|\delta_l\|^2 \leq V(\delta) \leq \bar{\alpha} \|\delta_l\|^2 \quad (48)$$

holds for

$$\underline{\alpha}(\gamma) = \kappa(\gamma) \min_{(i,j) \in \mathcal{E}} \{a_{ij}\} / 2, \quad \bar{\alpha} = \max_{(i,j) \in \mathcal{E}} \{a_{ij}\} / 2. \quad (49)$$

Proof: For any $|u| \leq \gamma < \pi$ and $|x| \leq \delta_l$, one has

$$\frac{\sin(u+x) - \sin x}{u} \leq 1. \quad (50)$$

Applying (V-B) and (50) yields

$$\begin{aligned} V(\delta) &= \frac{1}{2} \sum_{i=1}^n \sum_{j=1}^n a_{ij} \int_0^{\delta_i - \delta_j} \frac{\sin(u + \theta_{ij}^o) - \sin \theta_{ij}^o}{u} u du \\ &\geq \frac{1}{2} \sum_{i=1}^n \sum_{j=1}^n a_{ij} \int_0^{\delta_i - \delta_j} \kappa(\gamma) u du = \frac{1}{2} \kappa(\gamma) \delta^T B A_v B^T \delta \end{aligned}$$

and

$$V(\delta) \leq \frac{1}{2} \delta^T B A_v B^T \delta$$

Noting $\delta_l = B^T \delta$, the proof is complete. ■

Lemma 5.3 shows that the energy function $V(\delta)$ is bounded by quadratic functions of $\|\delta_l\|$. Using $V(\delta)$ as the RPLF candidate, the synchronization condition in the sense of Definition 3.3 is presented by the following theorem with $B_l(\gamma) := \{\delta_l \in \mathbb{R}^{|\mathcal{E}|} \mid \|\delta_l\| \leq \gamma\}$.

Theorem 5.2: Consider power systems (8) with energy function (47) under Assumption 3.1. Let $\gamma \in [0, \pi - 2\bar{\delta}_l)$ and $\kappa(\gamma)$ be defined in (26). Let function $\sigma(\gamma)$ be

$$\sigma(\gamma) := \frac{\|A_v B^T D^{-1} p(t)\|_{[t_0, \infty]}}{\gamma \kappa^{\frac{5}{2}}(\gamma)} \left(\frac{\max_{(i,j) \in \mathcal{E}} \{a_{ij}\}}{\min_{(i,j) \in \mathcal{E}} \{a_{ij}\}} \right)^{\frac{3}{2}}. \quad (51)$$

Define

$$Q = A_v B^T D^{-1} B A_v \geq 0. \quad (52)$$

If it holds that

$$\lambda_s(Q) > \lambda_{cr} := \sigma(\gamma^*), \quad (53)$$

where $\lambda_s(Q)$ is the smallest non-zero eigenvalue of Q and γ^* satisfies

$$\kappa(\gamma^*) = \frac{5}{3} \cos(\gamma^* + \bar{\delta}_l), \quad (54)$$

then the synchronization in the sense of Definition 3.3 is achieved. In particular,

- there exists $0 < \gamma_{\min} < \gamma^*$ and $\gamma^* < \gamma_{\max} < \gamma_{\max}$ such that $\lambda_s(Q) = \sigma(\gamma_{\min})$, $\lambda_s(Q) = \sigma(\gamma_{\max})$ and $\lambda_s(Q) > \lambda_{cr}$ for $\gamma \in (\gamma_{\min}, \gamma_{\max})$;
- (Energy Perspective) $W(\chi)$ is a positively invariant set for any $\chi \in [f_{l, \min}, f_{r, \max}]$ where

$$f_{l, \min} = \gamma_{\min}^2 \kappa(\gamma_{\min}) \min_{(i,j) \in \mathcal{E}} \{a_{ij}\} / 2, \quad (55)$$

$$f_{r, \max} = \gamma_s^2 \kappa(\gamma_s) \min_{(i,j) \in \mathcal{E}} \{a_{ij}\} / 2, \quad (56)$$

where γ_s satisfies

$$\cos(\gamma_s + \bar{\delta}_l) = -\kappa(\gamma_s), \quad (57)$$

i.e., any trajectories δ starting within $x(t_o) \in W(\chi)$ where is ultimately contained in $W(f_{l,\min})$;

C. (Angle Perspective: phase cohesiveness) let

$$\gamma_l = \gamma_{\min}, \gamma_r = \gamma_s \sqrt{\kappa(\gamma_s) \frac{\min_{(i,j) \in \mathcal{E}} \{a_{ij}\}}{\max_{(i,j) \in \mathcal{E}} \{a_{ij}\}}}. \quad (58)$$

Then, any trajectories δ starting within $B_l(\gamma)$ for $\gamma \in [\gamma_l, \gamma_r]$ is ultimately contained in $B_l(\gamma_l)$.

D. (Frequency Boundedness) if p is bounded, there exists a T such that $\|\delta\|_\infty \leq \varpi_o$ for some ϖ_o and $t > T$. \blacksquare

Proof: Let us consider Lyapunov function (47) within $\|\delta_l\| \leq \gamma$ for $\gamma \in [0, \pi - 2\bar{\delta}_l]$. The derivative of $V(\delta)$, along the trajectory of (8), is

$$\begin{aligned} \dot{V}(\delta) &= \frac{1}{2} \sum_{i=1}^n \sum_{j=1}^n a_{ij} (\sin(\delta_i - \delta_j + \theta_{ij}^o) - \sin \theta_{ij}^o) (\dot{\delta}_i - \dot{\delta}_j) \\ &= S(\delta) + Q(\delta) \end{aligned} \quad (59)$$

where $S(\delta)$ and $Q(\delta)$ are denoted as

$$\begin{aligned} S(\delta) &= \frac{1}{2} \sum_{i=1}^n \sum_{j=1}^n a_{ij} (\sin(\delta_i - \delta_j + \theta_{ij}^o) - \sin \theta_{ij}^o) \\ &\times \left\{ -d_i^{-1} \sum_{k=1}^n a_{ik} (\sin(\delta_i - \delta_k + \theta_{ik}^o) - \sin(\theta_{ik}^o)) \right. \\ &\left. + d_j^{-1} \sum_{k=1}^n a_{jk} (\sin(\delta_j - \delta_k + \theta_{jk}^o) - \sin(\theta_{jk}^o)) \right\} \end{aligned}$$

and

$$Q(\delta) = \frac{1}{2} \sum_{i=1}^n \sum_{j=1}^n a_{ij} (\sin(\delta_i - \delta_j + \theta_{ij}^o) - \sin \theta_{ij}^o) (d_i^{-1} p_i - d_j^{-1} p_j)$$

A manipulation of the indices in $S(\delta)$ leads to

$$\begin{aligned} S(\delta) &= - \sum_{i=1}^n \frac{1}{d_i} \left\{ \sum_{j=1}^n a_{ij} (\sin(\delta_i - \delta_j + \theta_{ij}^o) - \sin \theta_{ij}^o) \right\} \times \\ &\left\{ \sum_{j=1}^n a_{ij} (\sin(\delta_i - \delta_j + \theta_{ij}^o) - \sin \theta_{ij}^o) \right\} \end{aligned} \quad (60)$$

The RHS of the last equality in (60) equals to

$$S(\delta) = -\delta^T B A_p A_v B^T D^{-1} B A_v A_p B^T \delta$$

where A_p is a diagonal matrix with diagonal elements being

$$A_p(k, k) = \frac{\sin(\delta_i - \delta_j + \theta_{ij}^o) - \sin \theta_{ij}^o}{\delta_i - \delta_j},$$

for $(i, j) = \mathcal{E}_k, k = 1, \dots, |\mathcal{E}|$. It is noted from (V-B) that $A_p(k, k) \geq \kappa(\gamma)$, when $|\theta_j^o - \theta_i^o| \leq \delta_l$ and $|\delta_i(t) - \delta_j(t)| < \gamma$ for any $(i, j) \in \mathcal{E}$. One has

$$\begin{aligned} \delta^T B A_p A_v B^T D^{-1} B A_v A_p B^T \delta &= \xi^T \bar{Q} \xi \\ &\geq \|\xi\|^2 \min_{\xi \neq 0} \frac{\xi^T \bar{Q} \xi}{\xi^T \xi}. \end{aligned} \quad (61)$$

where $\xi = (A_v A_p)^{\frac{1}{2}} B^T \delta$ and $\bar{Q} = (A_p A_v)^{\frac{1}{2}} B^T D^{-1} B (A_v A_p)^{\frac{1}{2}}$. Note that \bar{Q} is the symmetric matrix whose eigenvalues are all non-negative. Let v be the eigenvector corresponding to the zero eigenvalue of \bar{Q} . We note that $v \in \text{null}(\bar{Q}) \in \text{null}(B(A_v A_p)^{\frac{1}{2}})$, since $\bar{Q}v = 0$ implies $B(A_v A_p)^{\frac{1}{2}}v = 0$. Also, $\xi \in \text{imag}((A_v A_p)^{\frac{1}{2}} B^T)$ which shows that $\xi \perp v$, because the null space of $B(A_v A_p)^{\frac{1}{2}}$ is orthogonal complement to the column space of $(A_v A_p)^{\frac{1}{2}} B^T$. Then, by Courant-Fischer minimum-maximum theorem, one has

$$\min_{\xi \neq 0} \frac{\xi^T \bar{Q} \xi}{\xi^T \xi} = \min_{\xi \neq 0, \xi \perp v} \frac{\xi^T \bar{Q} \xi}{\xi^T \xi} = \lambda_s(\bar{Q})$$

where $\lambda_s(\bar{Q})$ is the smallest non-zero eigenvalue of \bar{Q} . Also, $\|\xi\|^2 \geq \kappa(\gamma) \min_{(i,j) \in \mathcal{E}} \{a_{ij}\} \|\delta_l\|^2$ by noting $\delta_l = B^T \delta$. Due to $\bar{Q} = (A_v^{-1} A_p)^{\frac{1}{2}} Q (A_v^{-1} A_p)^{\frac{1}{2}}$, $\lambda_s(\bar{Q}) \geq \lambda_s(Q) \kappa(\gamma) / \max_{(i,j) \in \mathcal{E}} \{a_{ij}\}$ by Lemma 5.2. From (61),

$$\begin{aligned} \delta^T B A_p A_v B^T D^{-1} B A_v A_p B^T \delta &\geq \\ \frac{\min_{(i,j) \in \mathcal{E}} \{a_{ij}\}}{\max_{(i,j) \in \mathcal{E}} \{a_{ij}\}} \lambda_s(Q) \kappa^2(\gamma) \|\delta_l\|^2 \end{aligned}$$

Also one has $Q(\delta)$ in (59)

$$\begin{aligned} Q(\delta) &= \frac{1}{2} \sum_{i=1}^n \sum_{j=1}^n a_{ij} \frac{(\sin(\delta_i - \delta_j + \theta_{ij}^o) - \sin \theta_{ij}^o)}{\delta_i - \delta_j} (\delta_i - \delta_j) \\ &\times (d_i^{-1} p_i - d_j^{-1} p_j) = \delta^T B A_v A_p B^T D^{-1} p \\ &\leq \|A_v B^T D^{-1} p(t)\|_{[t_0, \infty]} \|\delta_l\| \end{aligned}$$

due to $\|A_p\| < 1$, Thus, \dot{V} is bounded by

$$\begin{aligned} \dot{V} &\leq -\kappa^2(\gamma) \lambda_s(Q) \frac{\min_{(i,j) \in \mathcal{E}} \{a_{ij}\}}{\max_{(i,j) \in \mathcal{E}} \{a_{ij}\}} \|\delta_l\|^2 \\ &+ \|A_v B^T D^{-1} p(t)\|_{[t_0, \infty]} \|\delta_l\| \\ &\leq 0, \text{ if } \|\delta_l\| \geq \frac{\|A_v B^T D^{-1} p(t)\|_{[t_0, \infty]} \max_{(i,j) \in \mathcal{E}} \{a_{ij}\}}{\lambda_s(Q) \kappa^2(\gamma) \min_{(i,j) \in \mathcal{E}} \{a_{ij}\}} \end{aligned} \quad (62)$$

So far, we proved that V is a RPLF. Then, if

$$g(\gamma) := \gamma \kappa^{\frac{5}{2}}(\gamma) / R_s > 1, \quad (63)$$

where

$$R_s := \left(\frac{\max_{(i,j) \in \mathcal{E}} \{a_{ij}\}}{\min_{(i,j) \in \mathcal{E}} \{a_{ij}\}} \right)^{\frac{3}{2}} \frac{\|A_v B^T D^{-1} p(t)\|_{[t_0, \infty]}}{\lambda_s(Q)} \quad (64)$$

the condition of Lemma 4.1 is satisfied. We further analyze the inequality (63) using Lemma 4.2. Note that $g(\gamma)$ in (41) is a quasi-sinusoidal function by Lemma 5.1 and maximizes at γ^* which satisfies (54). If $g(\gamma^*) > 1$ which is equivalent to (53), it follows from Lemma 4.2 that Statement A is satisfied with $\gamma_{\min} < \pi/2 - \bar{\delta}_l$ (by Lemma 5.1). We calculate $f_l(\gamma)$ as follows

$$f_l(\gamma) = \frac{\|A_v B^T D^{-1} p(t)\|_{[t_0, \infty]}^2 (\max_{(i,j) \in \mathcal{E}} \{a_{ij}\})^3}{2 \lambda_s^2(Q) \kappa^4(\gamma) (\min_{(i,j) \in \mathcal{E}} \{a_{ij}\})^2}$$

It is a monotonically increasing function of γ , because $\kappa(\gamma)$ is a monotonically decreasing function by Lemma 5.1. As a result, $f_{l,\min} = f_l(\gamma_{\min})$. We can obtain the neat expression of

$f_{l,\min}$ in (55) by noting $\lambda_s(Q) = \sigma(\gamma_{\min})$. We can calculate $f_r(\gamma) = \gamma^2 \kappa(\gamma) \min_{(i,j) \in \mathcal{E}} \{a_{ij}\}/2$. By Lemma 5.1,

$$\arg \max_{\gamma \in [\gamma_{\min}, \gamma_{\max}]} \{\gamma^2 \kappa(\gamma)\} = \gamma_s,$$

where γ_s satisfies (57). Thus, Statement B follows. Applying Lemma 4.2 shows γ_l is $\gamma_l = \gamma_{\min}$. Then, Statement C follows from that of Lemma 4.2 by noting that the function $\bar{\alpha}$ does not depend on γ . Statement D about frequency boundedness can easily follow from similar argument in Theorem 5.1 by noting that the system trajectory is ultimately contained in $B(\gamma_l)$, i.e., $\|\delta_l\| \leq \gamma_l = \gamma_{\min} \leq \pi/2 - \bar{\delta}_l$. ■

VI. EXTENSION TO NON-DISTURBANCE CASE: REGION OF ATTRACTION

In this section, we will extend the regional stability analysis method presented in Section IV and stability analysis in Section V-B and V-C to the non-disturbance case, i.e., $p = 0$ in (8). These results can be utilized to estimate the region of attraction for power systems (8), which is useful to assess the stability of power systems following severe faults such as tripping of a line. We first derive a variant of Lemma 4.2 when the derivative of the RPLF $V(x)$ satisfies (14) with $\mu(\gamma) = 0$.

Lemma 6.1: Consider nonlinear system (12) with regional Lyapunov function satisfying (13) and (14) with $\mu(\gamma) = 0$. Then,

- A. (Energy Perspective) $W(\chi)$ is a positively invariant set for any $\chi \in [0, f_{r,\max}]$ where

$$f_{r,\max} = \max_{\gamma \in [0, \gamma_m]} \{\gamma^2 \underline{\alpha}(\gamma)\}, \quad (65)$$

i.e., any trajectories starting within $x(t_o) \in W(\chi)$ ultimately converge to equilibrium point.

- B. (State Perspective) let

$$\gamma_r = \max_{\gamma \in [0, \gamma_m]} \left\{ \sqrt{\frac{f_{r,\max}}{\bar{\alpha}(\gamma)}} \mid \frac{f_{r,\max}}{\bar{\alpha}(\gamma)} \leq \gamma^2 \right\}. \quad (66)$$

Then, any trajectories starting within $B(\gamma_r)$ for $\gamma \in [0, \gamma_r]$ ultimately converge to equilibrium point, i.e., the region of attraction is $\|x\| \leq \gamma_r$. ■

Proof: Note that $f_r(\gamma) > f_l(\gamma)$ in Lemma 4.1 holds for all $\gamma \in [0, \gamma_m]$, since $\mu(\gamma) = 0$. The proof easily follows from that of Lemma 4.1 and 4.2 by setting $\mu(\gamma) = 0$. ■

Then, we can use Lemma 6.1 to show the next two theorems.

Theorem 6.1: Consider microgrid (8) with $p(t) = 0$ and energy function (31).

- A. (Energy Perspective) $W(\chi)$ is a positively invariant set for any $\chi \in [0, f_{r,\max}]$ where

$$f_{r,\max} = (\pi - \bar{\delta}_m)^2 \min_{i \neq j} \{d_i d_j\} / (2d), \quad (67)$$

where $\bar{\delta}_m$ is given in Theorem 5.1, i.e., any trajectories starting within $x(t_o) \in W(\chi)$ ultimately converge to equilibrium subspace \mathbb{E} ;

- B. (Angle Perspective) let

$$\gamma_r = (\pi - \bar{\delta}_m) \sqrt{\frac{\min_{i \neq j} \{d_i d_j\}}{\max_{i \neq j} \{d_i d_j\}}}, \quad (68)$$

Then, any trajectories starting within $B_c(\gamma)$ for $\gamma \in [0, \gamma_r]$ ultimately converge to equilibrium subspace \mathbb{E} , i.e., the region of attraction is $\|B_c^T \delta\| \leq \gamma_r$. ■

Proof: Note that the derivative of $V(\delta)$, along the trajectory of (8), is

$$\dot{V} \leq -\frac{\lambda_2}{n} \kappa(\gamma) \|\delta_c\|^2.$$

Then, the result follows from Lemma 6.1 and Theorem 5.1. ■

Theorem 6.2: Consider microgrid (8) with $p(t) = 0$ and energy function (47).

- A. (Energy Perspective) $W(\chi)$ is a positively invariant set for any $\chi \in [0, f_{r,\max}]$ where

$$f_{r,\max} = \gamma_s^2 \kappa(\gamma_s) \min_{(i,j) \in \mathcal{E}} \{a_{ij}\} / 2, \quad (69)$$

where γ_s satisfies (57), i.e., any trajectories starting within $x(t_o) \in W(\chi)$ where ultimately converge to equilibrium subspace \mathbb{E} ;

- B. (Angle Perspective) let

$$\gamma_r = \gamma_s \sqrt{\kappa(\gamma_s) \frac{\min_{(i,j) \in \mathcal{E}} \{a_{ij}\}}{\max_{(i,j) \in \mathcal{E}} \{a_{ij}\}}}, \quad (70)$$

Then, any trajectories starting within $B_l(\gamma)$ for $\gamma \in [0, \gamma_r]$ ultimately converge to equilibrium subspace \mathbb{E} , i.e., the region of attraction is $\|B^T \delta\| \leq \gamma_r$. ■

Proof: Note that the derivative of $V(\delta)$, along the trajectory of (8), is

$$\dot{V} \leq -\kappa^2(\gamma) \lambda_s(Q) \frac{\min_{(i,j) \in \mathcal{E}} \{a_{ij}\}}{\max_{(i,j) \in \mathcal{E}} \{a_{ij}\}} \|\delta_l\|^2 \quad (71)$$

Then, the result follows from Lemma 6.1 and Theorem 5.2. ■

Remark 6.1: When a fault occurs, we need to assure that the power system remains stable after the fault is cleared. The time duration between the fault occurrence and fault clearance is called critical clearing time. If the fault is cleared before the fault-on trajectories reach the boundaries of the region of attraction in Theorem 6.1 and 6.2, the trajectories can converge back to equilibrium subspace \mathbb{E} again. Therefore, we can use Theorem 6.1 and 6.2 to calculate the critical clearing time for power systems, which will be demonstrated in Section VII. ■

VII. NUMERICAL SIMULATION

Consider lossless microgrids in the network structure of IEEE 9-bus test system illustrated in Fig. 2. Buses 1, 2, 3 are the inverter-interfaced energy sources while the other buses are load buses. The numerical simulation will compare two algebraic stability conditions (33) and (53) given in Theorem 5.1 and 5.2, respectively. Both conditions are sufficient

TABLE I
TRANSMISSION LINE PARAMETERS AND NOMINAL POWER PROFILE p_i^o

line parameters (per unit)	a_{14}	a_{45}	a_{56}	a_{36}	a_{67}	a_{78}	a_{82}	a_{89}	a_{94}
a_{ij} (set 1)	17.2376	10.7036	5.8484	17.1069	9.8343	13.6459	15.8972	6.0142	11.3837
a_{ij} (set 2)	8.4148	10.6607	9.9044	10.1356	12.2033	10.6274	13.6683	9.5708	11.3565
bus number i	1	2	3	4	5	6	7	8	9
θ_i^o (rad, set 1)	0.1162	0.2195	0.1406	0.0483	0.0089	0.0909	0.0634	0.1168	0
θ_i^o (rad, set 2)	0.1841	0.1994	0.1269	0.0446	0	0.0429	0.0163	0.0799	0.0009
p_i^o (per unit)	1.17	1.63	0.85	-0.2	-0.9	-0.1	-1	-0.2	-1.25

conditions for the synchronization. We will use two sets of line parameters a_{ij} and show that one condition is not necessarily better than the other but they complement each other for predicting the stability and estimating the region of attraction. Two sets of line parameters a_{ij} and the nominal power profile $p_o = \text{col}\{p_1^o, \dots, p_n^o\}$ are given in Table. I. Note that $\max_{(i,j) \in \mathcal{E}} \{a_{ij}\} / \min_{(i,j) \in \mathcal{E}} \{a_{ij}\} = 1.6243$ in set 2 compared with $\max_{(i,j) \in \mathcal{E}} \{a_{ij}\} / \min_{(i,j) \in \mathcal{E}} \{a_{ij}\} = 2.9474$ in set 1, showing line parameters in set 2 are more evenly distributed across the network than set 1. The solutions θ_o to power flow equation (5) can be calculated and illustrated in Table. I. As a result, θ_l in (11) is $\theta_l = 0.2195$ rad for set 1 and $\theta_l = 0.1395$ rad for set 2. The system parameter d_i is randomly generated within range $d_i \in [0.7, 1]$.

We will emulate two scenarios: the time-varying disturbance scenario with $p \neq 0$ and line tripping scenario with $p = 0$ in (8). First, for $t \in [0, 5)$ s, since the equilibrium point is locally stable, we allow angles to settle to the equilibrium subspace \mathbb{E} . For the time-varying disturbance scenario, after $t = 5$ s, a random disturbance is injected at bus 1 to emulate the power generation fluctuation for renewable power. The disturbance will change its value randomly every 0.1 s, but its magnitude is bounded, i.e., $\sup_{t \in [0, \infty)} |p(t)| < p_d$ for some constant p_d . For line tripping scenario, at $t = 5$ s, we assume the electric line connecting bus 1 and 4 trips causing the system instability and making system trajectory leaves the equilibrium subspace \mathbb{E} . Theorem 6.1 and Theorem 6.2 give two estimation of region of attraction, namely $\|B_c \delta\| \leq \gamma_r$ for γ_r in (68) and $\|B \delta\| \leq \gamma_r$ for γ_r in (70). When both conditions $C_1 : \|B_c \delta\| \geq \gamma_r$ and $C_2 : \|B \delta\| \geq \gamma_r$ are triggered, we immediately re-close the line and retain the origin system structure making system trajectory converge to the equilibrium subspace \mathbb{E} again. We denote T_1 and T_2 as the time when C_1 and C_2 are triggered, respectively. In fact, T_1 and T_2 are the critical clearing time based on estimation of region of attraction given by Theorem 6.1 and Theorem 6.2. Note that the larger critical clearing time is more desirable, which allows more time for the protection system to take actions.

For time-varying disturbance scenario with parameter set 1, we set disturbance level $p_d = 1.0$, one can calculate $\lambda_2 = 4.0147$ and $\lambda_{cr} = 3.961$ such that the algebraic stability condition (33) is satisfied, while $\lambda_s(Q) = 32.6285$ and $\lambda_{cr} = 47.5875$ which shows the algebraic stability condition (53) is not satisfied and hence gives more conservative stability result. For the line tripping scenario, one can calculate region of attraction from Theorem 6.1 and 6.2 and obtains two estimations $C_1 : \|B_c \delta\| \leq 2.3044$ and $C_2 : \|B \delta\| \leq 0.7115$,

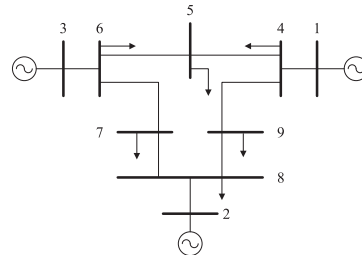


Fig. 2. Microgrids in 9-bus IEEE Test system structure

respectively. The numerical simulation shows that the critical clearing time $T_2 = 5.4658$ s and $T_1 = 5.6167$ s at which the line is re-connected, concluding that the stability result in terms of Definition 3.3 is more conservative than Definition 3.2. The simulation result is illustrate in Fig. 3.

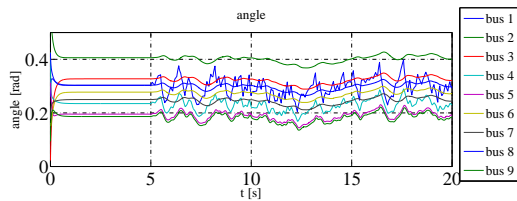
For time-varying disturbance scenario with parameter set 2, we set disturbance level $p_d = 5.0$, one can calculate $\lambda_s(Q) = 48.5049$ and $\lambda_{cr} = 45.6904$ such that the algebraic stability condition (53) is satisfied, while $\lambda_2 = 4.5773$ and $\lambda_{cr} = 45.6904$ which shows the algebraic stability condition (33) is not satisfied and hence gives more conservative stability result. For the line tripping scenario, one can calculate the region of attraction from Theorem 6.1 and 6.2 and obtains two estimations $C_1 : \|B_c \delta\| \leq 2.2684$ and $C_2 : \|B \delta\| \leq 0.9393$, respectively. The numerical simulation shows that the critical clearing time $T_1 = 5.6002$ s and $T_2 = 5.6439$ s, concluding that the stability result in terms of Definition 3.2 is more conservative than Definition 3.3. The simulation result is illustrate in Fig. 4.

VIII. CONCLUSION

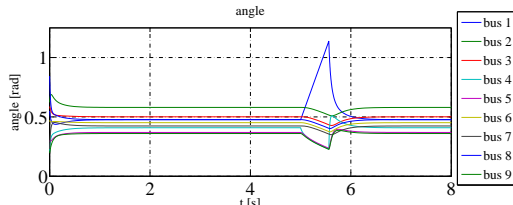
In this paper, we first presented the first-order power system model which coincides with non-uniform Kuramoto oscillators. Then, we introduced two definitions of stability in terms of phase cohesiveness and frequency boundedness. We proposed the stability analysis framework based on the RPLF and applied it to derive stability conditions in terms of two proposed stability definitions. Finally, we explicitly gave the estimation of region of attraction for microgrids. The effectiveness of the theoretical analysis is verified by the numerical simulation.

APPENDIX

Proof of Lemma 4.1: Since $V(x)$ is a RPLF satisfying (13) and (14), $V(x)$ decreases outside the ball $B(\mu(\gamma))$. In

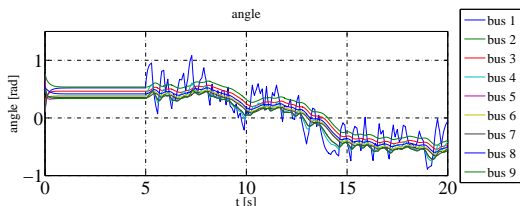


(a) Time-varying disturbance scenario.

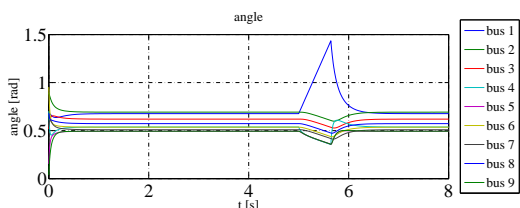


(b) Line tripping scenario.

Fig. 3. Simulation for parameter set 1.



(a) Time-varying disturbance scenario.



(b) Line tripping scenario.

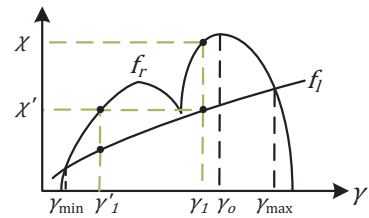
Fig. 4. Simulation for parameter set 2.

fact, $B(\mu(\gamma))$ is contained in $W(\chi)$, which follows from $x \in B(\mu(\gamma)) \Rightarrow x \in W(f_l(\gamma)) \Rightarrow x \in W(\chi)$ due to $\chi \geq f_l(\gamma)$. Therefore, one has $\dot{V} < 0$ at the boundary of $W(\chi)$ and hence $W(\chi)$ is an invariant set, i.e., any trajectories starting with $x \in W(\chi)$ will converge to and stay in $W(f_l(\gamma))$. The above argument is based on the argument $\|x\| \leq \gamma$ (the requirement for the existence of the RPLF). Next, we will show the condition $\|x(t)\| \leq \gamma$ holds for $t \geq t_o$ which is true if $\chi \leq f_r(\gamma)$, due to

$$\underline{\alpha}(\gamma)\|x(t)\|^2 \leq V(x(t)) \leq \chi \leq f_r(\gamma). \quad (72)$$

Hence, if $f_r(\gamma) \geq f_l(\gamma)$ or equivalently (15) holds, it is guaranteed that the invariant set $W(\chi)$ within which $\|x(t)\| \leq \gamma$ can be found. The proof is thus complete. ■

Proof of Lemma 4.2: We will prove $A \Rightarrow B \Rightarrow C$.

Fig. 5. The relation between $f_l(\gamma)$ and $f_r(\gamma)$.

$\Rightarrow A$. It is very straightforward to verify Statement A when $g(\gamma)$ is a quasi-sinusoidal function. In the rest of the proof, we consider functions $g(\gamma)$, $f_l(\gamma)$ and $f_r(\gamma)$ within the range $\gamma \in [\gamma_{\min}, \gamma_{\max}]$.

$A \Rightarrow B$. Statement A implies that $f_l(\gamma) \leq f_r(\gamma)$ for $\gamma \in [\gamma_{\min}, \gamma_{\max}]$, $f_l(\gamma_{\min}) = f_r(\gamma_{\min})$ and $f_l(\gamma_{\max}) = f_r(\gamma_{\max})$. By Lemma 4.1, $\chi \in [f_l(\gamma), f_r(\gamma)]$ whose maximum range is $[f_{l,\min}, f_{r,\max}]$ as γ varies within $\gamma \in [\gamma_{\min}, \gamma_{\max}]$. The relation between $f_l(\gamma)$ and $f_r(\gamma)$ is schematically illustrated in Fig. 5. For any $\chi \in [f_{l,\min}, f_{r,\max}]$, one can find $\gamma_1 = \arg \min_{\gamma \in [\gamma_{\min}, \gamma_{\max}]} \{f_r(\gamma) = \chi\}$. Since $f_l(\gamma_1) \leq \chi \leq f_r(\gamma_1)$, applying Lemma 4.1 shows any trajectories starting within $x \in W(\chi)$ is ultimately contained in the invariant set $W(f_l(\gamma_1))$. Set $\chi' = f_l(\gamma_1) \geq f_l(\gamma_{\min})$ and repeat the above argument with χ replaced by $\chi' < \chi$ and find γ'_1 . It is noted χ' and γ'_1 until $\chi' = f_l(\gamma_{\min})$. This search pattern is illustrated in Fig. 5. Then, we can prove the trajectory is eventually contained in set $W(f_l(\gamma_{\min}))$. Statement B is proved.

$B \Rightarrow C$. Due to (13), $\bar{\alpha}(\gamma)\|x\|^2 \leq f_{r,\max}$ implies $V \leq f_{r,\max}$, which shows that $B(\sqrt{f_{r,\max}/\bar{\alpha}(\gamma)}) \in W(f_{r,\max})$, i.e., any trajectory starts inside the ball $B(\sqrt{f_{r,\max}/\bar{\alpha}(\gamma)})$ is also inside $W(f_{r,\max})$. The size of the ball $B(\sqrt{f_{r,\max}/\bar{\alpha}(\gamma)})$ depends on the choice of γ and is required to be smaller than γ (the requirement of the RPLF for us to use (13)). We need to seek such ball of the largest size inside $W(f_{r,\max})$, which is equivalent to find γ_r in (17). As a result, $B(\gamma_r) \in W(f_{r,\max})$.

We can use similar argument to obtain γ_l . Because $V \leq f_{l,\min}$ implies $\underline{\alpha}(\gamma)\|x\|^2 \leq f_{l,\min}$, one has $W(f_{l,\min}) \in B(\sqrt{f_{l,\min}/\underline{\alpha}(\gamma)})$, i.e., any trajectory entering $W(f_{l,\min})$ also enters the ball $B(\sqrt{f_{l,\min}/\underline{\alpha}(\gamma)})$. The size of the ball $B(\sqrt{f_{l,\min}/\underline{\alpha}(\gamma)})$ depends on the choice of γ and is also required to be smaller than γ . We need to seek such ball of the smallest size that encloses $W(f_{l,\min})$, which is equivalent to find γ_l in (17). As a result, $W(f_{l,\min}) \in B(\gamma_l)$. Then, the statement C follows from statement B. ■

REFERENCES

- [1] N. Ainsworth and S. Grijalva. A structure-preserving model and sufficient condition for frequency synchronization of lossless droop inverter-based AC networks. *IEEE Transactions on Power Systems*, 28(4):4310–4319, 2013.
- [2] A. Amir-Moéz. Extreme properties of eigenvalues of a hermitian transformation and singular values of the sum and product of linear transformations. *Duke Mathematical Journal*, 23(3):463–476, 1956.
- [3] B.D.O. Anderson. Stability of control systems with multiple nonlinearities. *Journal of the Franklin Institute*, 282(3):155–160, 1966.
- [4] T. Athay, R. Podmore, and S. Virmani. A practical method for the direct analysis of transient stability. *IEEE Transactions on Power Apparatus and Systems*, (2):573–584, 1979.

- [5] A. Bergen and D. Hill. A structure preserving model for power system stability analysis. *IEEE Transactions on Power Apparatus and Systems*, (1):25–35, 1981.
- [6] H. Chang, C. Chu, and G. Cauley. Direct stability analysis of electric power systems using energy functions: theory, applications, and perspective. *Proceedings of the IEEE*, 83(11):1497–1529, 1995.
- [7] H. Chiang and C. Chu. Theoretical foundation of the BCU method for direct stability analysis of network-reduction power system. models with small transfer conductances. *IEEE Transactions on Circuits and Systems I: Fundamental Theory and Applications*, 42(5):252–265, 1995.
- [8] N. Chopra and M. Spong. On exponential synchronization of Kuramoto oscillators. *IEEE Transactions on Automatic Control*, 54(2):353–357, 2009.
- [9] S. Chung and J. Slotine. On synchronization of coupled Hopf-Kuramoto oscillators with phase delays. In *49th IEEE Conference on Decision and Control*, pages 3181–3187, 2010.
- [10] F. Dörfler and F. Bullo. On the critical coupling for Kuramoto oscillators. *SIAM Journal on Applied Dynamical Systems*, 10(3):1070–1099, 2011.
- [11] F. Dörfler and F. Bullo. Synchronization and transient stability in power networks and nonuniform Kuramoto oscillators. *SIAM Journal on Control and Optimization*, 50(3):1616–1642, 2012.
- [12] F. Dörfler, J.W. Simpson-Porco, and F. Bullo. Breaking the hierarchy: Distributed control and economic optimality in microgrids. *IEEE Transactions on Control of Network Systems*, 3(3):241–253, 2016.
- [13] A. El-Abiad and K. Nagappan. Transient stability regions of multimachine power systems. *IEEE Transactions on Power Apparatus and Systems*, (2):169–179, 1966.
- [14] A. Franci, A. Chaillet, and W. Pasillas-Lépine. Phase-locking between Kuramoto oscillators: robustness to time-varying natural frequencies. In *49th IEEE Conference on Decision and Control*, pages 1587–1592, 2010.
- [15] D. Hill and A. Bergen. Stability analysis of multimachine power networks with linear frequency dependent loads. *IEEE Transactions on Circuits and Systems*, 29(12):840–848, 1982.
- [16] D. Hill and G. Chen. Power systems as dynamic networks. In *IEEE International Symposium on Circuits and Systems*, pages 722–725, 2006.
- [17] D. Hill and C. Chong. Lyapunov functions of Lur’e-Postnikov form for structure preserving models of power systems. *Automatica*, 25(3):453–460, 1989.
- [18] Z. Huang, S. Jin, and R. Diao. Predictive dynamic simulation for large-scale power systems through high-performance computing. In *High Performance Computing, Networking, Storage and Analysis (SCC)*, pages 347–354, 2012.
- [19] A. Jadbabaie, N. Motee, and M. Barahona. On the stability of the Kuramoto model of coupled nonlinear oscillators. In *Proceedings of American Control Conference*, volume 5, pages 4296–4301, 2004.
- [20] P. Kundur, N. Balu, and M. Lauby. *Power system stability and control*, volume 7. McGraw-hill New York, 1994.
- [21] R. H. Lasseter. MicroGrids. In *IEEE Power Engineering Society Winter Meeting*, volume 1, pages 305–308, 2002.
- [22] G.A. Lüders. Transient stability of multimachine power systems via the direct method of Lyapunov. *IEEE Transactions on Power Apparatus and Systems*, (1):23–36, 1971.
- [23] R. Majumder. Some aspects of stability in microgrids. *IEEE Transactions on power systems*, 28(3):3243–3252, 2013.
- [24] Z. Miao, A. Domijan, and L. Fan. Investigation of microgrids with both inverter interfaced and direct ac-connected distributed energy resources. *IEEE Transactions on Power Delivery*, 26(3):1634–1642, 2011.
- [25] I. Nagel, L. Fabre, M. Pastre, F. Krümmenacher, R. Cherkaoui, and M. Kayal. High-speed power system transient stability simulation using highly dedicated hardware. *IEEE Transactions on Power Systems*, 28(4):4218–4227, 2013.
- [26] P. Piagi and R.H. Lasseter. Autonomous control of microgrids. In *Power Engineering Society General Meeting, 2006. IEEE*, pages 8–pp. IEEE, 2006.
- [27] J. Schiffer, R. Ortega, A. Astolfi, J. Raisch, and T. Sezi. Conditions for stability of droop-controlled inverter-based microgrids. *Automatica*, 50(10):2457–2469, 2014.
- [28] J. Schiffer, T. Seel, J. Raisch, and T. Sezi. Voltage stability and reactive power sharing in inverter-based microgrids with consensus-based distributed voltage control. *IEEE Transactions on Control Systems Technology*, 24(1):96–109, 2016.
- [29] J.W. Simpson-Porco, F. Dörfler, and F. Bullo. Droop-controlled inverters are kuramoto oscillators. *IFAC Proceedings Volumes*, 45(26):264–269, 2012.
- [30] J.W. Simpson-Porco, F. Dörfler, and F. Bullo. Synchronization and power sharing for droop-controlled inverters in islanded microgrids. *Automatica*, 49(9):2603–2611, 2013.
- [31] M. Verwoerd and O. Mason. On computing the critical coupling coefficient for the Kuramoto model on a complete bipartite graph. *SIAM Journal on Applied Dynamical Systems*, 8(1):417–453, 2009.
- [32] L. Zhu and D. Hill. Transient stability analysis of power systems: A network perspective (accepted for SIAM Journal on Control and Optimization). 2018.
- [33] L. Zhu and D.J. Hill. Transient stability analysis of microgrids with network-preserving structure. In *6th IFAC Workshop on Distributed Estimation and Control in Networked Systems*, 2016.